NANOPARTICLES WITH AGGREGATION-INDUCED EMISSION FOR MONITORING LONG TIME CELL MEMBRANE INTERACTIONS

Hao Cheng[1, 4], Wei Qin[2], Zhenfeng Zhu[1], Jun Qian[1], Anjun Qin[3], Ben Zhong Tang[2], and Sailing He[1, 4, 5, *]

[1]Centre for Optical and Electromagnetic Research, Zhejiang Provincial Key Laboratory for Sensing Technologies, JORCEP (Joint Research Center of Photonics of the Royal Institute of Technology, Lund University and Zhejiang University), Zijingang Campus, Zhejiang University (ZJU), Hangzhou 310058, China

[2]Department of Chemistry, The Hong Kong University of Science & Technology, Clear Water Bay, Kowloon, Hong Kong, China

[3]Department of Polymer Science and Engineering, Zhejiang University, Hangzhou 310027, China

[4]ZJU-SCNU Joint Research Center of Photonics, South China Academy of Advanced Optoelectronics, South China Normal University (SCNU), Guangzhou 510006, China

[5]Department of Electromagnetic Engineering, Royal Institute of Technology, Stockholm 10044, Sweden

Abstract—We perform the long time monitoring of nanoparticle-cell membrane interaction with high spatial and temporal resolution. The 2, 3-bis(4-(phenyl(4-(1, 2, 2-triphenylvinyl) phenyl)amino)phenyl) fumaronitrile (TPE-TPA-FN) is doped in organically modified silica (ORMOSIL) to be a biocompatible nanoprobe, which displays an aggregation-induced emission (AIE) effect. Photobleaching resistance of this synthesized nanoparticle is tested and compared with its similar counterpart, which proves its superiority and capability of long term fluorescence emission. We utilize the objective-based total internal reflection microscopy combined with the living cell incubation platform to investigate the cell uptake process of this nanoparticle in real time.

1. INTRODUCTION

A majority of organic fluorophores that are highly emissive in solution show weak or no light emission in the solid state due to the aggregation formation in the condensed phase [1]. Aggregation formation induces the light emission quenching from the π-π stacking in many π-conjugated fluorophores, and this is notoriously known as aggregation-caused quenching (ACQ) [2]. In bio-imaging technology nowadays, fluorophore-doped nanoparticles with their various advantages [2] have emerged as a novel imaging contrast agent. However, the photophysical phenomenon of ACQ obstructs the capability of increasing the fluorophore-doped concentration in nanoparticles as a brighter emitter for bio-imaging. Many approaches have been taken to control this effect, which are usually accompanied by some side effects such as the steric effects and electronic effects [3]. Fortunately, a novel class of fluorophores have been discovered and display the opposite effect; they show no emission in dilute solutions but are brightly fluorescent upon concentration or solidification [4]. The so-called aggregation-induced emission (AIE) feature of this kind of fluorophores has been extensively studied. Based on the understanding of the AIE mechanism, novel nanoparticles have been designed and have shown their versatility in various application areas, including fluorescence imaging, biosensing, organic light-emitting diodes, etc. [5]. Since the AIE effect allows a higher concentration of fluorophores to be loaded in a single nanoprobe, it makes the AIE solutions more emissive and photobleaching-resistant as well [5]. Therefore, in comparison to normal ACQ materials, AIE materials are endowed with diverse benefits in laser-induced *in vivo* biological imaging and investigation, where lower average excitation power and long term observation is demanded. In addition, the cytotoxicity test experiments also support the biocompatibility of this type of materials [6], making it a more desirable bioprobe than the inorganic quantum dots (QDs).

Total internal reflection fluorescence microscopy (TIRFM) is based on the principle of evanescent wave (EW) excited emission [7]. This electromagnetic energy is generated at the interface of two kinds of medium with different refractive indexes. It decays exponentially from the boundary of the medium of lower refractive index. Usually, the penetration depth of EW is of the order of the excitation light wavelength (50 nm $\sim$ 250 nm) [8, 9] and varies accompanied with the angle adjustment of total reflection. Because of this thin film excitation, only the fluorophores close enough to the interface could be excited, and the out-of-focus fluorescence is suppressed to a large extent. Therefore, it enables a sub-wavelength imaging

resolution perpendicular to the interface, which conveniently allows
for the real-time monitoring of cell surface events and minimizes the
photodamage of the cell. In microscopy systems, TIRFM is commonly
realized in two types: the prism-based type and the objective-based
type [7].   Though comparatively complicated, the objective-based
type shows its advantages with sample-top accessibility, higher light
collection efficiency and better image quality [10], which makes it
more flexible and stable in biological application. In this geometry,
an objective lens of high numerical aperture (> 1.4) [11] is utilized
for both excitation and signal collection. When in combination with
a conventional inverted fluorescence microscopy system, it permits
the direct observation and manipulation of specimens located on the
surface of the coverslip or cell culture dish. With all these specific
advantages, TIRFM offers a desirable platform for studying the cell
membrane of a living cell in the nanoscale area.

In this paper, we use the organically modified silica (ORMOSIL)
nanoparticles to encapsulate the AIE-active 2, 3-bis(4-(phenyl(4-(1,
2, 2-triphenylvinyl)phenyl)amino) phenyl) fumaronitrile (TPE-TPA-
FN) aggregates based on the techniques developed from our former
works [12–14]. This kind of nanoparticle displays aggregation enhanced
fluorescence as desired. Photobleaching resistance of this material
has been tested both *in vitro* and in living cells, which proves its
beneficial effect of long term bright emission. To take advantage of
its excellent features, we combine it with the TIRFM system to enable
the monitoring of the interaction between the nanoparticle and the
cell membrane at a located region. Real time images are achieved and
discussed to unravel its potentiality in emerging biological applications.

2. MATERIALS AND METHODS

2.1. Synthesis of the AIE Nanoparticles

Figure 1 shows the synthesis procedure of the TPE-TPA-FN
doped ORMOSIL nanoparticles in the nonpolar core of Aerosol-
OT/DMF/water micelles.   Briefly, the micelles were prepared by
dissolving a certain amount of Aerosol-OT and 1-butanol in 10 ml of DI
water through vigorous magnetic stirring. 200 µl of TPE-TPA-FN in
DMF were then added to the solution under magnetic stirring. Half an
hour later, 100 µl of neat VTES were added to the micellar system, and
the resulting solution was stirred for about 1 hour. Next, ORMOSIL
nanoparticles were precipitated by adding 10 µl of APTES and stirred
for another 20 h at room temperature. After the formation of the
nanoparticles, surfactant Aerosol-OT, cosurfactant 1-butanol, residual
VTES and APTES were removed by dialyzing the solution against DI
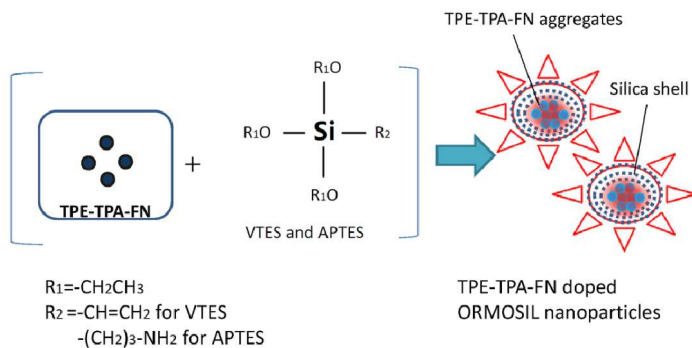
Figure 1. Schematic illustration of the AIE nanoparticles used in this study.

water in a 12–14 kDa cutoff cellulose membrane for 50 h. The dialyzed solution was then filtered through a 0.45 μm cutoff membrane filter to be used in later experiments.

In the control group for the bleaching test, the TPE-TPA-FN was replaced by Nile Red, a type of dye which would bear the ACQ effect, and encapsulated in the same way. A detailed method can be referred to Ref. [14].

2.2. TIRFM for Living Cell Investigation

Figure 2 gives the representative configuration of our imaging system. The Olympus IX71 inverted microscope with an optical fiber-based
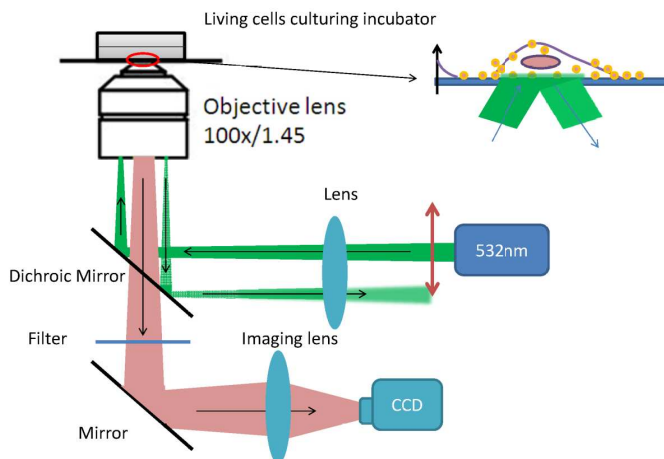
Figure 2. Configuration of TIRFM system.

TIRFM accessory is used for light excitation. A 532 nm single mode laser (MSL 30 mW, CNI) is coupled and aligned into the laser optical path, where a power density of 200 μw/mm^2 is achieved. The fiber light exit point is fixed to the conjugate plane of the back focal plane of the high numerical aperture TIRF objective lens (Olympus PLAPO100XOTIRFM, N.A. 1.45). Then the system enables the simple operation switching between TIRF and wide-field (WF) illumination through the adjusting of relative position between the laser path and the optical central axis of the system. To achieve TIR illumination, a droplet of match oil ($n = 1.518$) is smeared between the objective lens and the bottom of a special dish. The evanescent wave illumination is obtained at the interface between the dish bottom and the cell culture environment when the laser pathway is tilted enough to surpass the critical angle ($\sim$normally 62° under this circumstance). Real-time images are collected by the same objective lens and then captured by the color CCD camera (Pro-microscan, OPLENIC). To separate the fluorescence emission from excitation background, a dichroic mirror and a high pass filter (U-MNIG, Olympus) are used.

Under the experiment for monitoring the nanoparticles-cell membrane interaction process in TIRF, a CO_2 incubation system for microscopes (Olympus MIU-IBC) is mounted on the stage of the inverted microscope and the live images are captured by the EMCCD camera (iXon3 885, Andor) with fast speed and high contrast.

2.3. Cell Culture

HeLa cells were cultivated in Dulbecco's minimum essential media (DMEM) with 10% fetal bovine serum (FBS), 1% penicillin, and 1% amphotericin B at 37° in the humidified atmosphere under 5% CO_2. The cells were seeded in special 6 cm dishes, of which the bottom has been replaced by a coverslip with thickness of $\sim$ 0.17 mm to enable observation under the TIRF objective lens. After growth for 24 h, the diluted TPE-TPA-FN doped ORMOSIL nanoparticles solution was added to a final concentration of 12.5 μg/ml in the culture medium. The same concentration of Nile red doped ORMOSIL nanoparticles solution was added in the control experiment, and all samples were incubated for another 2 h. Afterwards, the cells were gently washed thrice by phosphate buffered saline (PBS, pH = 7.4, 10 mM) and imaged by microscopy under 532 nm light excitation.

When conducting the real-time TIRF experiment, the cells were washed after 5 min incubation and quickly transferred to the small incubator mounted on the microscope. Here the cells could be kept in a stable 37° environment throughout the experiments by three heater

modules in combination with heating of the objective lens, which was in direct thermal contact with the bottom of the dish. Tubes for the supply of CO_2 were also available to control the CO_2 level for long time experiments.

3. RESULT AND DISCUSSION

3.1. Characterization of the AIE Nanoparticles

The TEM image (Fig. 3(a)) shows the uniform spherical shape and an average size of about 20 nm for these nanoparticles. The silica encapsulation provides a stable optical transparent protection for the organic dyes and could be functionalized further for specific biological applications [14]. Fig. 3(b) shows the UV absorption and Fluorescence spectra (532 nm excited) of the nanoparticles. Excitonic and emission peaks are located at 510 nm and 630 nm respectively. The nanoparticles dispersed in the aqueous solution give a pink color and does not show any significant discolor or sediment for months, indicating its chemical stability.


(a)   (b)
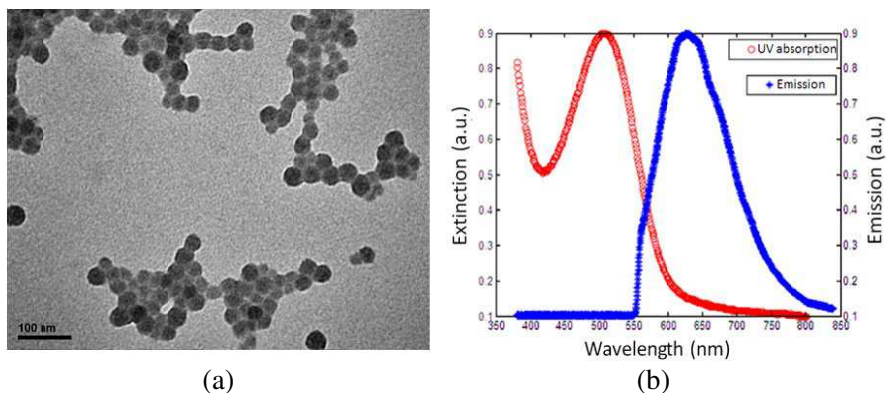
Figure 3. (a) TEM picture, (b) the UV absorption and fluorescence emission spectrum of the TPE-TPA-FN doped ORMOSIL nanoparticles.

3.2. Photobleaching Resistance of AIE Nanoparticles

We test the photobleaching resistance of this synthesized AIE nanoparticle in this section, in order to to envision its feature of long-term monitoring for biological application.

3.2.1. Single Particle Bleaching Test

The diluted dye solution was dried and dispersed on a cleared coverslip and then illuminated persistently by the 532 nm laser in WF. The intensity image stack was achieved by the color CCD camera every 10 seconds. The result is shown in Fig. 4. The fluorescence intensity of the single isolated nanoparticle decreases along with the illumination lasting time, which is displayed as the imaging spot fading in the image series. The single nanoparticle fluorescence bleaching characteristic could be calculated through the post-process with the image stack. We focus on one particle here, of which the intensity is the accumulation of all its corresponding image pixels. The decay curve illustrates the bleaching process with respect to time. It shows a photobleaching time of minute scale, which is comparably longer than most organic fluorophores.
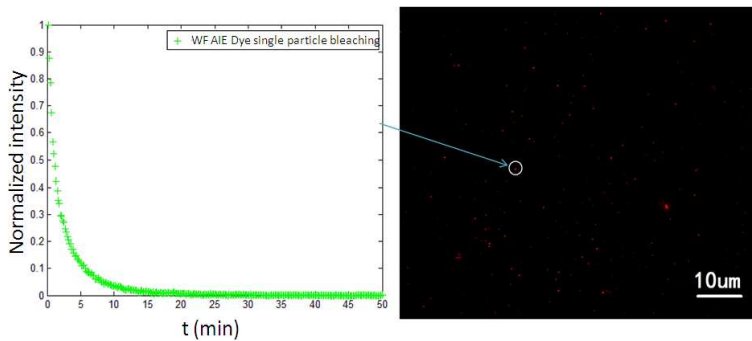
**Figure 4.** Photobleaching test of single AIE nanoparticle.

This single particle test demonstrates the long time emission capability of this kind of materials. In addition, it is predicted that if a higher concentration of the aggregates is encapsulated in by the silica, the photobleaching resistance of this single nanoparticle could be strengthened. It provides an alternative probe for the high sensitive fluorescence microscopy techniques, such as single particle tracking (SPT), which allows an improved temporal and spatial resolution for the cell-particle interaction detection [9].

3.2.2. Cell Labeling Bleaching Test Compared with ACQ Nanoparticles

Afterwards, we utilize this nanoparticle as an optical probe for cell imaging. Due to the cationic charges introduced by silica

encapsulation, nanoparticles could adhere to the cell membrane by electrostatic bonding. This rapid process occurred in less than 1 minute in our experiments and then until $\sim$ 5–10 minutes fluorescence was detectable from cytoplasm. By two more hours of cell culturing after adding the AIE nanoparticles, it could be confirmed that the labeling process was fully accomplished. In the control group, we prepared the sample with Nile red doped ORMOSIL nanoparticles solution in the same condition.

After a 2 h incubation, we gently wash both samples with PBS and examine them under our imaging system. Both nanoparticles exhibit their capability of cell labeling. And through a procedure similar to that for the single particle bleaching test, we compare
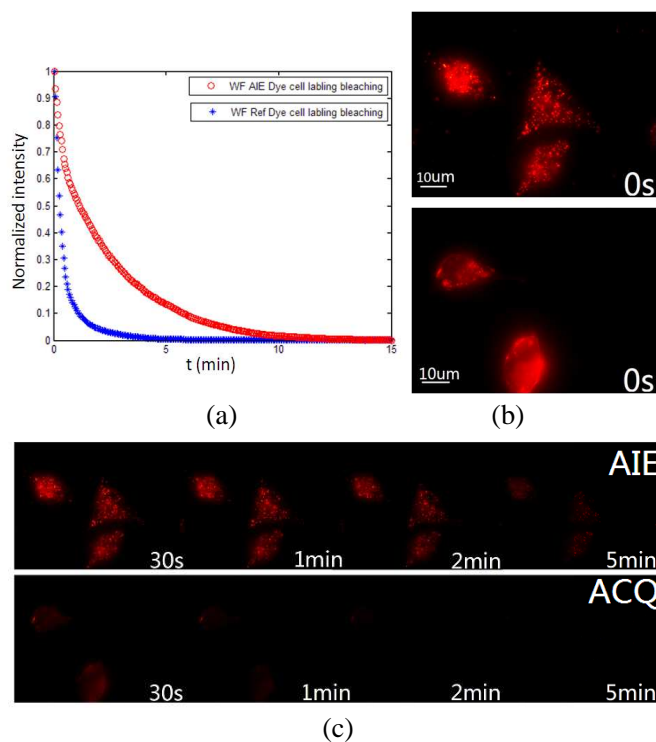

Figure 5.   Comparison between AIE nanoparticles and ACQ nanoparticles for cell imaging. (a) Illustrates the bleaching curves, (b) show WF cell labeling images with these two types of nanoparticles, (c) shows the time lapse bleaching processes of these two types of nanoparticles.

the photobleaching resistance of these two types of bioprobes. As
shown in Fig. 5, under the same excitation and collection condition,
the imaging intensity decreases rapidly in the control group, while
remains detectable by the color CCD camera until 5 minutes after
AIE nanoparticles labeling.

3.3. Cellular Uptake Investigation with TIRF

The photobleaching resistance as well as the biocompatibility features
allow for the real time observation of the pathway and process of this
novel nanoparticle entering into the living cell.

The images captured in WF and TIRFM by the EMCCD camera
are compared in Fig. 6. In TIR mode, an image of higher signal to noise
ratio and contrast was achieved. Fewer nanoparticles were excited in
this mode due to the illumination selectivity by the evanescence wave,
and fluorescence from cytoplasm was suppressed.
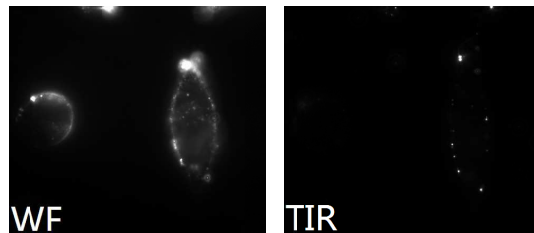
Figure 6. Cell imaging results with AIE nanoparticles in WF and
TIR modes, respectively.

The real time nanoparticles uptake process could be captured
by the EMCCD in video mode, and the compressed 40 minutes long
observation video could give a vivid display of the entire cell uptake
process. Here, only nanoparticles located near the basal membrane
area of the cell could be excited and imaged, and dim white light
is shined through the transmission mode to give the cell contour in
order to confirm that the variation of the nanoparticle image is due
to the interaction with the cell. At the beginning of our real time
monitoring, we optimize the position of the objective lens to focus
on the nanoparticles in the excitation area of the evanescence wave
As displayed in Fig. 7, the particle located at the membrane outline
exhibits a periodic fluorescence fluctuation at first (Phase 1), which
indicates its contact with the cell. It also moves slightly accompanied
by the creep movement of the single cell. Then, this particle becomes
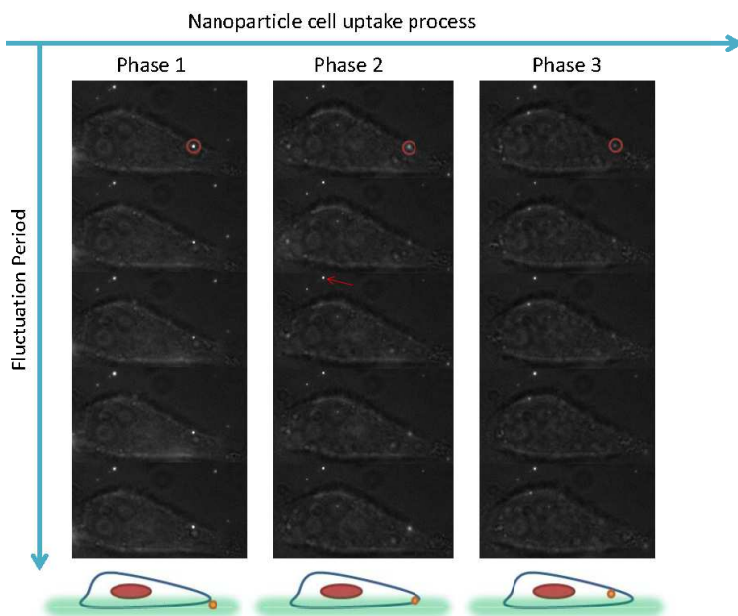
Figure 7. Typical AIE nanoparticle movement in cell membrane area (Nanoparticle in the red ring was excited by the evanescence wave and was monitored by TIRFM with the overlap of the cell contour; for reference, the red arrow indicated a fixed nanoparticle keeping focused during all the phases).

dim and displays as an out-of-focusing image while continuing the periodic fluctuation (Phase 2). For reference, some other particles located at some no-cell area (attached to the bottom of the culture dish and no transposition movement occurred during all the observation period) remain focused during the same time interval, which excludes the influence from the instability of imaging condition. Thus, the out-of-focusing image results from the entry of particles and then the gradual departure from the cell membrane's illuminated area. At last, the nanoparticle disappeared immediately from the field of view when it entered into the cell and diffused randomly in cytoplasm (Phase 3).

In Fig. 8, we study the single particle situation and focus on a single fluctuation period (see the inset of Fig. 8 at five different times) to monitor its interaction or diffusion movement on the cell membrane. It is noticeable that the nanoparticle fluorescence lasts longer than that in the former bleaching test experiment, due to the weaker excitation mode in TIR condition.
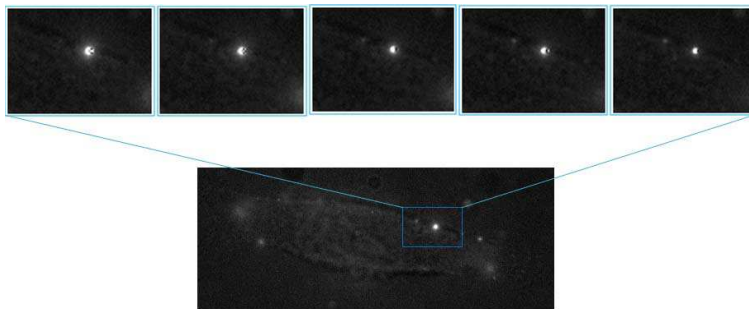
Figure 8. Nanoparticle-cell membrane interaction in details.

Though the TEM image shows that the single nanoparticle is of the size with the diffraction limit, we found that some of the single nanoparticle images captured by the EMCCD camera are not always a perfect spherical shape when it adhered to the cell membrane. It is acknowledged that a fluorescent molecule can be regarded as an electrical dipole [15]. And based on the previous research report, the intensity distribution of the deteriorated images contains information about the molecule or nanoparticle's emission dipole orientation [16]. Thus, the donut shapes could result from the orientation variation of the dye particle on the cell membrane, which indicated both the transitional and rotational diffusions during the cell uptake process of AIE nanoparticles.

4. CONCLUSION

The TPE-TPA-FN doped ORMOSIL nanoparticle has been shown in our study to be a photostable fluorescence organic bioprobe that is suitable for long-term monitoring of the cell-particle interaction. Since the ORMOSIL nanoparticle could be further functionalized with co-conjugated bio-molecules, it is a versatile probe for early diagnosis/therapy of cancer and other diseases [14]. In the last decade, along with the thriving of research in the single molecule and sub-wavelength level, the TIRFM system has been utilized and developed extensively. TIRFM has been used in technical innovations such as smFRET [17], TIR-FCS [10], SPT [9] for single molecule detection and SIM [18], STORM [19] for fluorescence super-resolution microscopy and these reflect its flexibility in the related research. The combination of both advantages of AIE nanoparticles and the TIRFM system provides a fresh optional cell tracing tool and allows for more detailed studies of biological process in this platform.

ACKNOWLEDGMENT

REFERENCES

1. Birks, J. B., *Photophysics of Aromatic Molecules*, 1970.
2. Qin, W., D. Ding, J. Z. Liu, W. Z. Yuan, Y. Hu, B. Liu, and B. Z. Tang, "Biocompatible nanoparticles with aggregation-induced emission characteristics as far-red/near-infrared fluorescent bioprobes for in vitro and in vivo imaging applications," *Adv. Funct. Mater.*, Vol. 22, No. 4, 771–779 2012.
3. Yuan, W. Z., P. Lu, S. M. Chen, J. W. Y. Lam, Z. M. Wang, Y. Liu, H. S. Kwok, Y. G. Ma, and B. Z. Tang, "Changing the behavior of chromophores from aggregation-caused quenching to aggregation-induced emission: Development of highly efficient light emitters in the solid state," *Adv. Mater.*, Vol. 22, No. 19, 2159, 2010.
4. Luo, J. D., Z. L. Xie, J. W. Y. Lam, L. Cheng, H. Y. Chen, C. F. Qiu, H. S. Kwok, X. W. Zhan, Y. Q. Liu, D. B. Zhu, and B. Z. Tang, "Aggregation-induced emission of 1-methyl-1, 2, 3, 4, 5-pentaphenylsilole," *Chem. Commun.*, No. 18, 1740–1741, 2001.
5. Hong, Y. N., J. W. Y. Lam, and B. Z. Tang, "Aggregation-induced emission: Phenomenon, mechanism and applications," *Chem. Commun.*, No. 29, 4332–4353, 2009.
6. Yu, Y., Y. N. Hong, C. Feng, J. Z. Liu, J. W. Y. Lam, M. T. Faisal, K. M. Ng, K. Q. Luo, and B. Z. Tang, "Synthesis of an AIE-active fluorogen and its application in cell imaging," *Sci. China Ser. B*, Vol. 52, No. 1, 15–19, 2009.
7. Axelrod, D., "Total internal reflection fluorescence microscopy in cell biology," *Traffic*, Vol. 2, No. 11, 764–774, 2001.
8. Jaiswal, J. K. and S. M. Simon, "Imaging single events at the cell membrane," *Nat. Chem. Biol.*, Vol. 3, No. 2, 92–98, 2007.
9. Ruthardt, N., D. C. Lamb, and C. Brauchle, "Single-particle tracking as a quantitative microscopy-based approach to unravel cell entry mechanisms of viruses and pharmaceutical nanoparticles," *Mol. Ther.*, Vol. 19, No. 7, 1199–1211, 2011.

10. Thompson, N. L. and B. L. Steele, "Total internal reflection with fluorescence correlation spectroscopy," *Nat. Protoc.*, Vol. 2, No. 4, 878–890, 2007.

11. Toomre, D. and J. Bewersdorf, "A new wave of cellular imaging," *Annu. Rev. Cell Dev. Bi.*, Vol. 26, 285–314, 2010.

12. Li, K., W. Qin, D. Ding, N. Tomczak, J. L. Geng, R. R. Liu, J. Z. Liu, X. H. Zhang, H. W. Liu, B. Liu, and B. Z. Tang, "Photostable fluorescent organic dots with aggregation-induced emission (AIE dots) for noninvasive long-term cell tracing," *Sci. Rep.*, Vol. 3, UK, 2013.

13. Wang, D., J. Qian, S. L. He, J. S. Park, K. S. Lee, S. H. Han, and Y. Mu, "Aggregation-enhanced fluorescence in PEGylated phospholipid nanomicelles for in vivo imaging," *Biomaterials*, Vol. 32, No. 25, 5880–5888, 2011.

14. Qian, J., X. Li, M. Wei, X. W. Gao, Z. P. Xu, and S. L. He, "Bio-molecule-conjugated fluorescent organically modified silica nanoparticles as optical probes for cancer cell imaging," *Opt. Express*, Vol. 16, No. 24, 19568–19578, 2008.

15. Lotito, V., U. Sennhauser C. V. Hafner, and G.-L. Bona, "Interaction of an asymmetric scanning near field optical microscopy probe with fluorescent molecules," *Progress In Electromagnetics Research*, Vol. 121, 281–299, 2011.

16. Bohmer, M. and J. Enderlein, "Orientation imaging of single molecules by wide-field epifluorescence microscopy," *J. Opt. Soc. Am. B*, Vol. 20, No. 3, 554–559, 2003.

17. Roy, R., S. Hohng, and T. Ha, "A practical guide to single-molecule FRET," *Nat. Methods*, Vol. 5, No. 6, 507–516, 2008.

18. Gustafsson, M. G. L., "Nonlinear structured-illumination microscopy: Wide-field fluorescence imaging with theoretically unlimited resolution," *Pro. Natl. Acad. Sci. USA*, Vol. 102, No. 37, 13081–13086, 2005.

19. Rust, M. J., M. Bates, and X. W. Zhuang, "Sub-diffraction-limit imaging by stochastic optical reconstruction microscopy (STORM)," *Nat. Methods*, Vol. 3, No. 10, 793–795, 2006.